



The following Communications have been judged by at least two referees to be “very important papers” and will be published online at www.angewandte.org soon:

Q. Wang, M. Zhang, C. Chen, W. Ma, J. Zhao*

Photocatalytic Aerobic Oxidation of Alcohols on TiO₂: The Acceleration Effect of a Brønsted Acids

Ye Fu, Q. Dai, W. Zhang, J. Ren, T. Pan,* C. He*

AlkB Domain of Mammalian ABH8 Catalyzes Hydroxylation of 5-Methoxycarbonylmethyluridine at the Wobble Position of tRNA

S. Rizzato, J. Bergès, S. A. Mason, A. Albinati, J. Kozelka*

Dispersion-Driven Hydrogen Bonding: Theoretically Predicted H-bond between H₂O and Platinum(II) Identified by Neutron Diffraction

H. Amouri,* J. Moussa, A. K. Renfrew, P. J. Dyson, M. N. Rager, L.-M. Chamoreau

Metal Complex of Diselenobenzoquinone : Discovery, Structure, and Anticancer Activity

M. Rauschenberg, S. Bomke, U. Karst, B. J. Ravoo*

Dynamic Peptides as Biomimetic Carbohydrate Receptors

M. Baer, D. Marx, G. Mathias*

Microsolvated Hydronium and Zundel Cations by Theoretical Messenger Spectroscopy

M. Roth, P. Kindervater, H.-P. Raich, J. Bargon, H. W. Spiess,* K. Münnemann*

Continuous ¹H and ¹³C Signal Enhancement in NMR and MRI Using Parahydrogen and Hollow Fiber Membranes

M. R. Leone, G. Lackner, A. Silipo, R. Lanzetta, A. Molinaro,* C. Hertweck*

An Unusual Galactofuranose Lipopolysaccharide Warrants Intracellular Survival of Toxin-Producing Bacteria in Their Fungal Host



“My favorite subjects at school were scientific subjects such as chemistry, biology, mathematics, and physics. I also liked philosophy.

The biggest problem that scientists face is financial support (and the time invested in getting it). ...”

This and more about Ramón Martínez-Máñez can be found on page 6708.

Author Profile

Ramón Martínez-Máñez — 6708

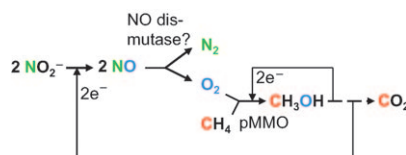
Modern Molecular Photochemistry of Organic Molecules

Nicholas J. Turro, V. Ramamurthy, Juan C. Scaiano

Books

reviewed by M. Fagnoni — 6709

More than one way to skin a cat: Some strictly anaerobic bacteria grow in the presence of methane and nitrite, forming CO₂ and N₂. Recently published experimental evidence suggests the involvement of a NO dismutase and of a particulate methane monooxygenase (pMMO) in the process. Both enzymes are lacking in microorganisms that catalyze anaerobic methane oxidation with sulfate. There are thus at least two pathways that enable anaerobes to use methane as fuel.



Highlights

Methane Oxidation

R. K. Thauer* — 6712–6713

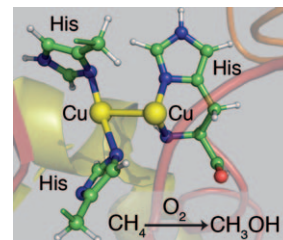
Functionalization of Methane in Anaerobic Microorganisms

Methane Monooxygenase

R. A. Himes, K. Barnese,
K. D. Karlin* — 6714–6716

One is Lonely and Three is a Crowd: Two
Coppers Are for Methane Oxidation

What/where is the active site? The determination of the metal ion content and makeup of the bacterial membrane protein methane monooxygenase (pMMO) has an enigmatic research history, despite protein X-ray structures. A new study appears to settle the issue; the dicopper center facilitates oxidation of methane to methanol. However, the unusual active-site environment leaves many questions for future investigations on the relevant copper-dioxygen chemistry and biochemistry.

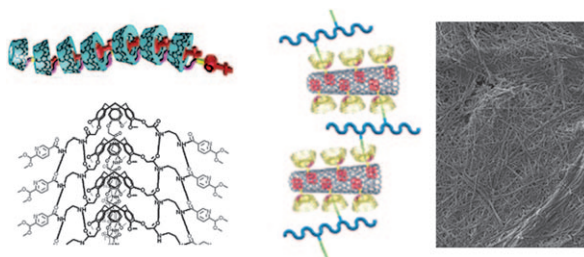


Minireviews

Cavitand Gelators

J. A. Foster, J. W. Steed* — 6718–6724

Exploiting Cavities in Supramolecular
Gels



Through the incorporation of cavities into supramolecular gelators, the well-established host–guest chemistry of cavitands can be utilized to build up and break down

gel structures, introduce responsive functionalities, and enhance selectivity in applications such as catalysis and extraction.

Reviews

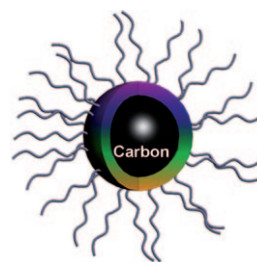
Nanotechnology

S. N. Baker,* G. A. Baker* — 6726–6744



Luminescent Carbon Nanodots:
Emergent Nanolights

A glowing review: Carbon nanodots have recently emerged as intriguing, cheap, sustainable, and low-toxicity nanoemitters that hold immense promise in energy conversion, bioimaging, diagnostics, and novel composites. This Review summarizes recent advances in the synthesis, understanding, and exploitation of carbon-based quantum dots as nascent biolabels, while pointing to potential new directions for this fascinating class of nanocarbon.



For the USA and Canada:
ANGEWANDTE CHEMIE International
Edition (ISSN 1433-7851) is published weekly
by Wiley-VCH, PO Box 191161, 69451 Wein-
heim, Germany. Air freight and mailing in the
USA by Publications Expediting Inc., 200
Meacham Ave., Elmont, NY 11003. Periodicals

postage paid at Jamaica, NY 11431. US POST-
MASTER: send address changes to *Angewandte
Chemie*, Journal Customer Services, John
Wiley & Sons Inc., 350 Main St., Malden,
MA 02148-5020. Annual subscription price for
institutions: US\$ 9442/8583 (valid for print and
electronic / print or electronic delivery); for

individuals who are personal members of a
national chemical society prices are available
on request. Postage and handling charges
included. All prices are subject to local VAT/
sales tax.

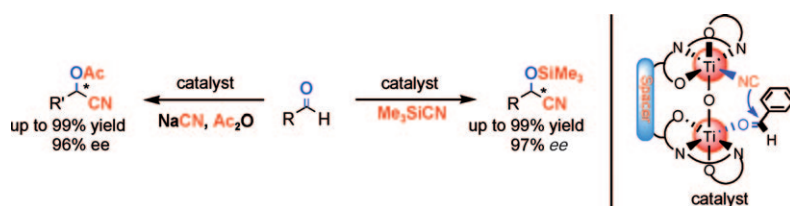
Communications

Synthetic Methods



Z. Zhang, Z. Wang, R. Zhang,
K. Ding* ————— 6746–6750

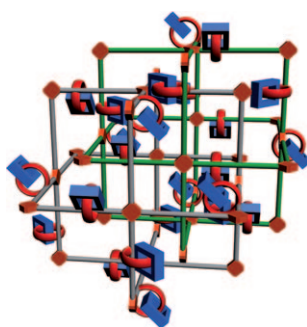
An Efficient Titanium Catalyst for
Enantioselective Cyanation of Aldehydes:
Cooperative Catalysis



Two-in-one: The integration of two salen/ $\text{Ti}=\text{O}$ units into one molecule allows the enantioselective cyanation of aldehydes to afford the enantioenriched natural or nonnatural cyanohydrin derivatives with

turnover numbers of 1960–172 000 and *ee* values up to 97 % (see scheme). Some of the cyanohydrin derivatives are key intermediates for the synthesis of chiral pharmaceuticals or agrochemicals.

MIMs meet MOFs: Mechanically interlocked molecules (MIMs), in the form of donor–acceptor [2]catenane-containing struts of exceptional length, have been incorporated into a three-dimensional catenated metal–organic framework (MOF) at precise locations and with uniform relative orientations. Catenation is expressed simultaneously within the struts and the framework.

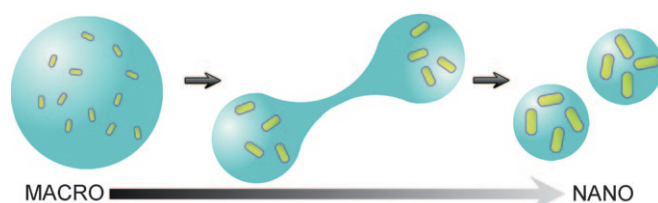


Metal–Organic Frameworks



Q. Li, C.-H. Sue, S. Basu, A. K. Shveyd,
W. Zhang, G. Barin, L. Fang,
A. A. Sarjeant, J. F. Stoddart,*
O. M. Yaghi* ————— 6751–6755

A Catenated Strut in a Catenated Metal–
Organic Framework



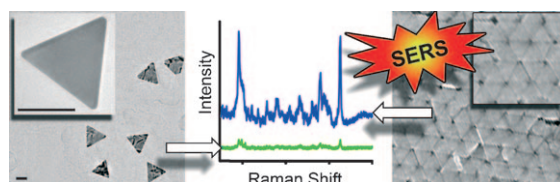
Divide yourselves! An interfacial reaction drives the spontaneous and sequential division of macroscopic droplets all the way into nanoscopic emulsions (see picture). The sizes of the divided droplets depend on the pH of the solution and the

division process is governed by the interplay between surface tension and electrostatic effects. When the dividing droplets contain nanoscopic cargo (e.g., nanorods), they partition it equally into progeny micelles.

Micelles

K. P. Browne, D. A. Walker,
K. J. M. Bishop,
B. A. Grzybowski* ————— 6756–6759

Self-Division of Macroscopic Droplets:
Partitioning of Nanosized Cargo into
Nanoscale Micelles



SERSly good! Crystallization of triangular gold nanoprism into close-packed mono- and multilayers is facilitated by electrostatic repulsions. The ordering of the

nanotriangles causes an order-of-magnitude increase in surface-enhanced Raman spectroscopy (SERS) enhancement relative to that of disordered assemblies.

Crystal Engineering

D. A. Walker, K. P. Browne, B. Kowalczyk,
B. A. Grzybowski* ————— 6760–6763

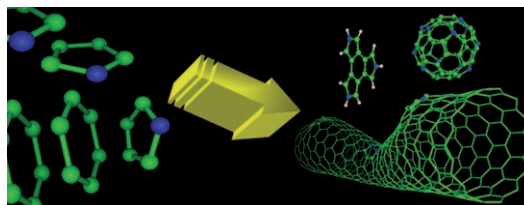
Self-Assembly of Nanotriangle
Superlattices Facilitated by Repulsive
Electrostatic Interactions

Heteroaromatics

X. Gao, S. B. Zhang,* Y. Zhao,
S. Nagase* — 6764–6767



A Nanoscale Jigsaw-Puzzle Approach to Large π -Conjugated Systems



Piecing the puzzle together: A simple model of stability for hybrid carbon-conjugated materials is revealed and computationally verified. Based on this model, a simple “jigsaw-puzzle” strategy towards

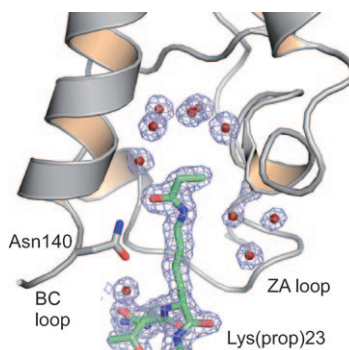
the design for a family of highly viable hybrid carbon-conjugated materials is proposed (see picture; C green, N blue, H white).

Epigenetics

F. Vollmuth, M. Geyer* — 6768–6772



Interaction of Propionylated and Butyrylated Histone H3 Lysine Marks with Brd4 Bromodomains



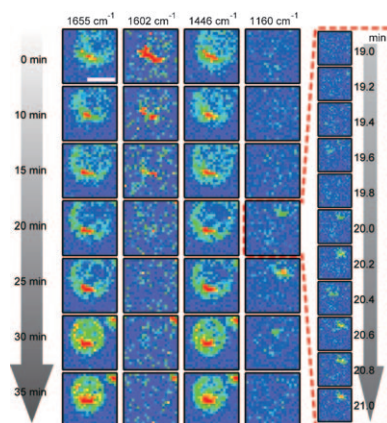
Recognized as sisters: Histone modifications determine the state of chromatin remodeling and gene activation. Lysine propionylation and butyrylation have been identified as new histone marks (besides acetylation) that expand the epigenetic code. The alignment of the additional methylene groups of such propionylated (see picture) and butyrylated lysine residues between a highly conserved Pro–Phe motif suggests a general mode of bromodomain recognition.

Chemical Bioimaging

M. Okuno, H. Kano,* P. Leproux,
V. Couderc, J. P. R. Day, M. Bonn,
H. Hamaguchi* — 6773–6777



Quantitative CARS Molecular Fingerprinting of Single Living Cells with the Use of the Maximum Entropy Method



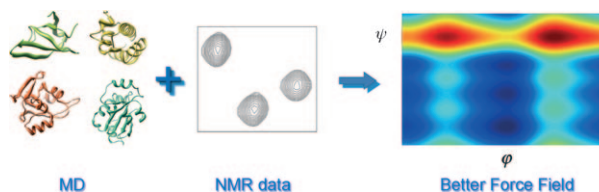
Fast CARS: The cell-death process was observed in real time at the subcellular level by coherent anti-Stokes Raman microspectroscopy, an extension of anti-Stokes Raman scattering (CARS) microscopy. Changes in the chemical contrast during the dying process can be clearly resolved (see picture).

Protein Dynamics

D. W. Li, R. Brüschweiler* — 6778–6780

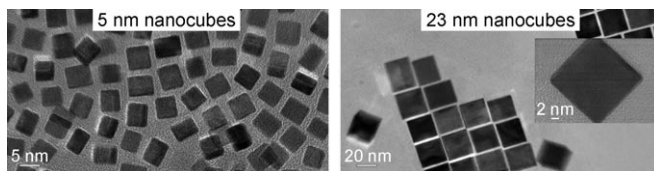


NMR-Based Protein Potentials



Speed training: A highly efficient screening of new potentials against the parent molecular dynamics (MD) trajectories of trial proteins provides a greater than 10^5 -fold increase in the speed of the analysis

by using a re-weighting scheme guided by experimental NMR data for proteins, thereby improving the accuracy of computer simulations of proteins.



Precision preparation: A facile, one-step, polyol protocol has been developed to prepare monodisperse, single-crystalline Au–Cu bimetallic nanocubes. Through the careful adjustment of the reaction

parameters, both the dimensions of the nanocubes (two examples with edge lengths of 23 and 5 nm are shown) and their gold and copper stoichiometry can be controlled.

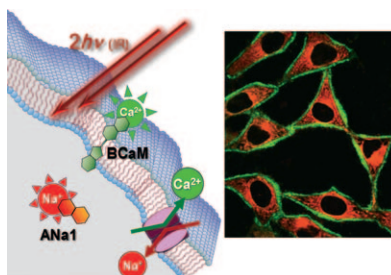
Nanostructures

Y. Liu,* A. R. H. Walker — 6781 – 6785

Monodisperse Gold–Copper Bimetallic Nanocubes: Facile One-Step Synthesis with Controllable Size and Composition



A two-photon probe (BCaM) shows 14-fold enhancement in two-photon emission fluorescence in response to Ca^{2+} and shows high sensitivity and selectivity for near-membrane Ca^{2+} ions (see picture). Combined with the known Na^+ two-photon probe ANa1, BCaM allows simultaneous dual-color imaging of $\text{Ca}^{2+}/\text{Na}^+$ activities within live cells and in tissues at more than 100 μm depth for long time periods without photobleaching.



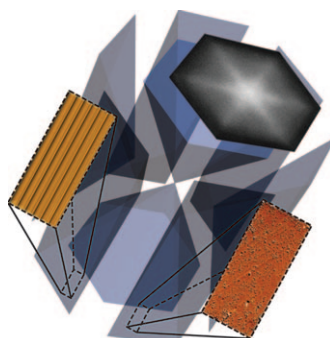
Two-Photon Fluorescent Probes

H. J. Kim, J. H. Han, M. K. Kim, C. S. Lim, H. M. Kim,* B. R. Cho* — 6786 – 6789

Dual-Color Imaging of Sodium/Calcium Ion Activities with Two-Photon Fluorescent Probes



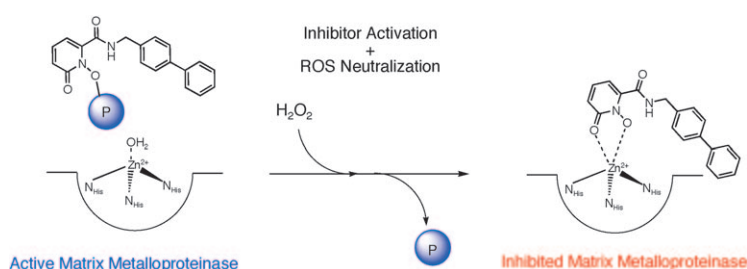
Starless molecular sieves: The starlike appearance of confocal fluorescence microscopy (CFM) images of large crystals of the AlPO-5 family of microporous materials is due to the presence of barriers to molecular diffusion in the internal crystal architecture (see picture) rather than a star-shaped subcrystal according to studies by CFM, focused ion beam milling, electron backscatter diffraction, and atomic force microscopy.



Molecular Sieves

L. Karwacki, H. E. van der Bij, J. Kornatowski, P. Cubillas, M. R. Drury, D. A. M. de Winter, M. W. Anderson, B. M. Weckhuysen* — 6790 – 6794

Unified Internal Architecture and Surface Barriers for Molecular Diffusion of Microporous Crystalline Aluminophosphates



Doing double duty: A metalloproteinase inhibitor that can be activated by reactive oxygen species (ROS) has been designed to protect the blood-brain barrier (BBB) in ischemic reperfusion injury. By both neu-

tralizing damaging ROS and inhibiting degradative metalloproteinases, a single compound can eliminate both threats to the BBB upon activation.

Metalloprotein Proinhibitors

J. L. Major Jourden, S. M. Cohen* — 6795 – 6797

Hydrogen Peroxide Activated Matrix Metalloproteinase Inhibitors: A Prodrug Approach



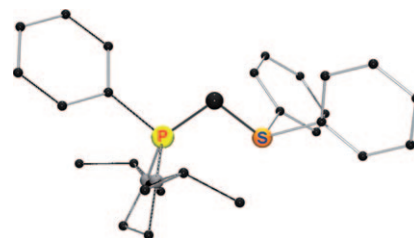
Atomic Carbon Sources

N. Dellus, T. Kato,* X. Bagán,
N. Saffon-Merceron, V. Branchadell,
A. Baceiredo* ————— **6798 – 6801**



An Isolable Mixed P,S-Bis(ylide) as an Asymmetric Carbon Atom Source

Heart of carbon: The first stable asymmetric bis(ylide), N,N' -(*i*-Pr₂NCH₂CH₂NiPr)(Ph)P–C–SPh₂, has been isolated (see picture; C black, N gray). The presence of the two different ligands causes this carbon(0) complex to behave as an asymmetric atomic carbon source.

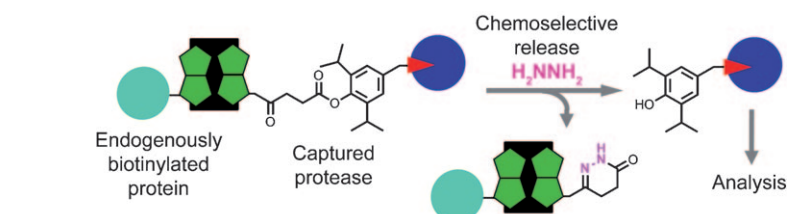


Proteomics

P. P. Geurink, B. I. Florea, N. Li,
M. D. Witte, J. Verasdonck, C.-L. Kuo,
G. A. van der Marel,
H. S. Overkleeft* ————— **6802 – 6805**



A Cleavable Linker Based on the Levulinoyl Ester for Activity-Based Protein Profiling



Get linked: The title linker is stable under various biological conditions and can be cleaved chemoselectively with hydrazine (see scheme). Its use is demonstrated in

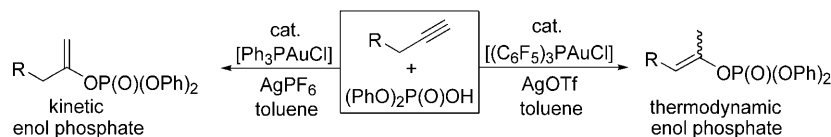
the activity-based enrichment and identification of proteasome active subunits from cell extracts.

Gold Catalysis

P. H. Lee,* S. Kim, A. Park, B. C. Chary,
S. Kim* ————— **6806 – 6809**



Gold(I)-Catalyzed Addition of Diphenyl Phosphate to Alkynes: Isomerization of Kinetic Enol Phosphates to the Thermodynamically Favored Isomers



Gold, gold, or ... gold? It depends on the (gold) catalyst whether the product of thermodynamic or kinetic control is formed in an unprecedented hydrophosphorylation approach to enol phosphates (see scheme). A third catalyst,

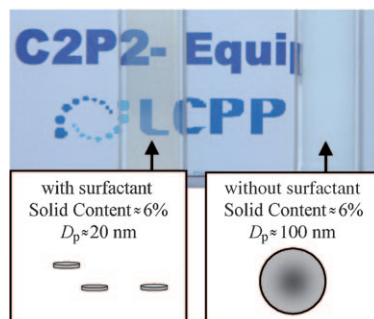
$[(C_6F_5)_3PAuOTf]$, was found to be exceedingly effective for the previously unknown isomerization of kinetic enol phosphates to the thermodynamically favored isomers. Tf = trifluoromethanesulfonyl; R = alkyl, cyclohexyl, Ph.

Emulsion Polymerization

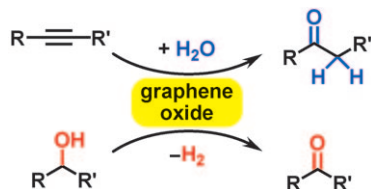
E. Grau, P.-Y. Dugas, J.-P. Broyer,
C. Boisson, R. Spitz,
V. Monteil* ————— **6810 – 6812**



Aqueous Dispersions of Nonspherical Polyethylene Nanoparticles from Free-Radical Polymerization under Mild Conditions



A radical idea: Free-radical polymerization of ethylene usually requires severe conditions. Here, the efficiency of this reaction was investigated under mild conditions (less than 250 bar) in water for the production of stable polyethylene (PE) aqueous dispersions (see picture, D_p = particle diameter). Latexes of PE nanoparticles with various shapes (cylinder or sphere) and solid contents up to 40% were prepared.

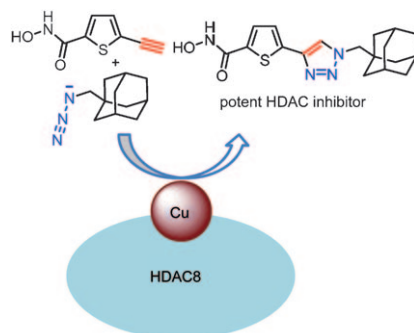


Do not pass GO: Graphene oxide (GO) catalyzes the oxidation of various alcohols and alkenes, and the hydration of various alkynes into their respective aldehydes and ketones in good to excellent yields. The reactions proceed under relatively mild conditions and simple filtration was shown to be a convenient and effective method of catalyst recovery.

Carbocatalysis

D. R. Dreyer, H.-P. Jia,
C. W. Bielawski* — 6813–6816

Graphene Oxide: A Convenient Carbocatalyst for Facilitating Oxidation and Hydration Reactions

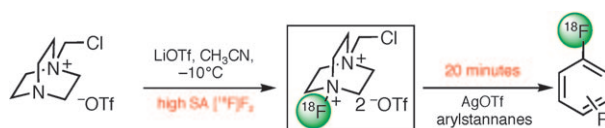


It all happened with a click: In a search for histone deacetylase (HDAC) inhibitors using in situ click chemistry, the first example of protein–Cu acceleration of the azide–alkyne cycloaddition reaction was uncovered. The copper center in the protein target HDAC8 catalyzed triazole formation between one azide–alkyne pair among 30 possibilities. These results provide a new route to HDAC inhibitors and a precedent for new types of protein-based catalysts for click chemistry.

Click Chemistry

T. Suzuki,* Y. Ota, Y. Kasuya, M. Mutsuga,
Y. Kawamura, H. Tsumoto, H. Nakagawa,
M. G. Finn,* N. Miyata* — 6817–6820

An Unexpected Example of Protein-Templated Click Chemistry



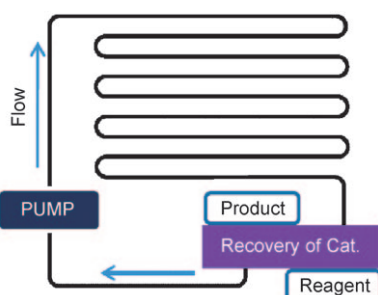
Selectfluor, one of the most reactive and commonly used electrophilic fluorinating N–F reagents, has been radiolabeled with ^{18}F . The resulting new ^{18}F -labeled N–F reagent is safe, nontoxic, and easy to handle. The combined use of

^{18}F Selectfluor bis(triflate) and AgOTf allows for the preparation of electron-rich ^{18}F -aromatic compounds through a simple “shake and mix” protocol at room temperature (see scheme; SA = specific activity).

Radiochemistry

H. Teare, E. G. Robins, A. Kirjavainen,
S. Forsback, G. Sandford, O. Solin,*
S. K. Luthra,*
V. Gouverneur* — 6821–6824

Radiosynthesis and Evaluation of ^{18}F Selectfluor bis(triflate)



Keep on running: A microchemical system for continuous flow catalytic reactions with a magnetic catalyst is presented (see picture). It enables the automatic separation and recirculation of catalyst particles and is applicable to various catalytic reactions.

Microreactors

C. P. Park, D.-P. Kim* — 6825–6829

A Microchemical System with Continuous Recovery and Recirculation of Catalyst-Immobilized Magnetic Particles

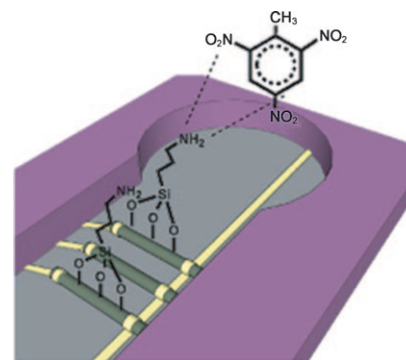
Sensors

Y. Engel, R. Elnathan, A. Pevzner,
G. Davidi, E. Flaxer,
F. Patolsky* ————— **6830–6835**



Supersensitive Detection of Explosives by
Silicon Nanowire Arrays

Dog on a chip: Explosives can be detected with unprecedented sensitivity by using arrays of silicon nanowire field-effect transistors modified with an electron-rich aminosilane monolayer, which form complexes with the analytes (see picture). These “nanosniffers” can be used to sense the presence of TNT at concentrations as low as 1×10^{-6} ppt, which is superior to that of sniffer dogs or any other known explosive detection method.

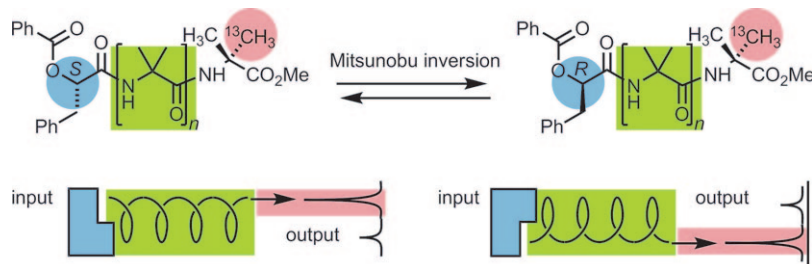


Conformational Communication

J. Solà, S. P. Fletcher, A. Castellanos,
J. Clayden* ————— **6836–6839**



Nanometer-Range Communication of
Stereochemical Information by Reversible
Switching of Molecular Helicity



A long-distance call: The inversion of configuration at a stereogenic center led to a detectable switch in the position of a ^{13}C stereochemical probe 40 bonds

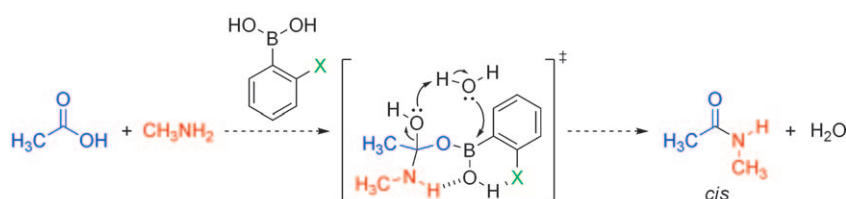
(2.5 nm) away. Information was relayed between the sites by an inversion of screw sense in the intervening helix as illustrated (^{13}C NMR signals were read as output).

Computational Chemistry

T. Marcelli* ————— **6840–6843**



Mechanistic Insights into Direct Amide
Bond Formation Catalyzed by Boronic
Acids: Halogens as Lewis Bases



Get the water out! DFT calculations predict water elimination from a tetrahedral intermediate to be the rate determining step in the title reaction. This transformation is calculated to be highly

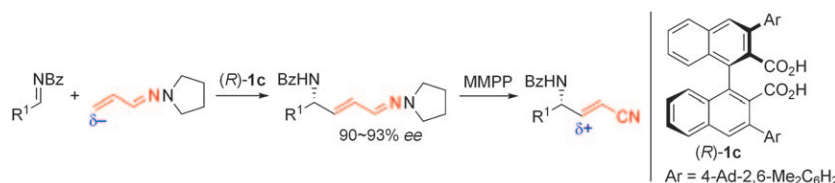
stereoselective, yielding *cis* amides as the kinetic products (see scheme). The superior activity of *ortho*-halophenyl boronic acids results from the Lewis basic character of halogen atoms.

Organocatalysis

T. Hashimoto, H. Kimura,
K. Maruoka* ————— **6844–6847**

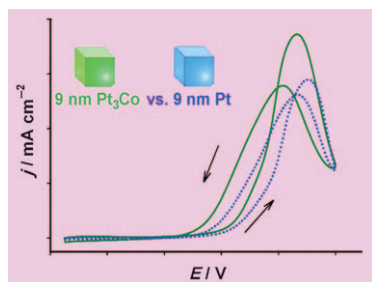


Enantioselective Formal Alkenylations of
Imines Catalyzed by Axially Chiral
Dicarboxylic Acid Using Vinylogous
Aza-Enamines



In the zone: The use of vinylogous aza-enamines (hydrazones) as a source of an alkenyl group has been achieved (see scheme). Unmasking of the aza-enamine moiety opens up a novel approach for the

preparation of chiral allylic amines bearing an electron-withdrawing alkene moiety functionalized at the electron-deficient β position.

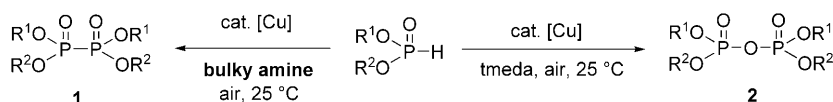


Loaded dice: High-quality and similarly sized Pt₃Co and Pt nanocubes were prepared by gradually reducing metal precursors at high temperatures. Cyclic voltammetric and chronoamperometric results show a much higher methanol oxidation current density on Pt₃Co nanocubes (see picture). The enhanced catalytic activity was explained by the slower and weaker adsorption of CO onto Pt₃Co.

Shape-Controlled Catalysts

H. Yang, J. Zhang, K. Sun, S. Zou,*
J. Fang* 6848–6851

Enhancing by Weakening:
Electrooxidation of Methanol on
Pt₃Co and Pt Nanocubes



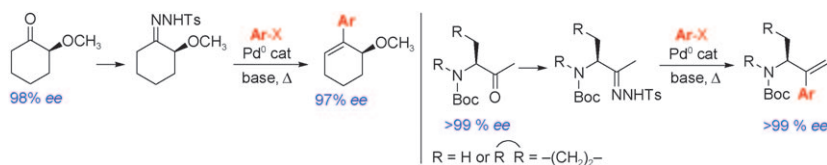
Different copper complexes selectively catalyze the aerobic oxidative coupling of H-phosphonates to afford either hypophosphates and pyrophosphates in high

yields with high selectivity (see scheme; tmeda = *N,N,N',N'*-tetramethylethylenediamine).

Coupling Reactions

Y. B. Zhou, S. F. Yin, Y. X. Gao, Y. F. Zhao,
M. Goto, L.-B. Han* 6852–6855

Selective P–P and P–O–P Bond
Formations through Copper-Catalyzed
Aerobic Oxidative Dehydrogenative
Couplings of H-Phosphonates



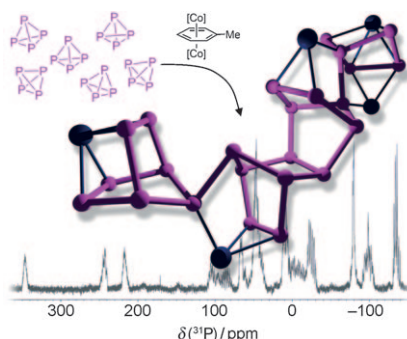
Papa was a rollin' ketone: Arylation of ketones with preservation of the chirality in configurationally unstable α -chiral ketones has been achieved by the palladium-catalyzed cross-coupling reaction

between tosylhydrazones and aryl halides (see scheme; Boc = *tert*-butoxycarbonyl, Ts = 4-toluenesulfonyl). The regioselectivity in the β -hydride elimination step is key for the retention of configuration.

Cross-Coupling

J. Barluenga,* M. Escribano, F. Aznar,
C. Valdés* 6856–6859

Arylation of α -Chiral Ketones by
Palladium-Catalyzed Cross-Coupling
Reactions of Tosylhydrazones with Aryl
Halides



Under control: Controlled self-aggregation of P₄ to extended neutral polyphosphorus cages was achieved in the presence of cobalt complex fragments. X-ray structure analyses of P₁₂, P₁₆, and P₂₄ ligand complexes give insights into the formation of aggregated allotropes of phosphorus from elemental P₄.

Phosphorus Cages

F. Dielmann, M. Sierka, A. V. Virovets,
M. Scheer* 6860–6864

Access to Extended Polyphosphorus
Frameworks



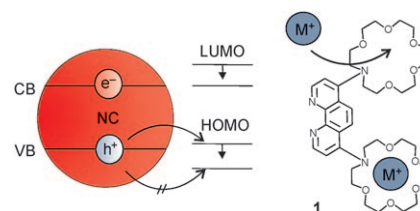
Quantum Dots

J. Völker, X. Zhou, X. Ma, S. Flessau,
H. Lin, M. Schmittle,
A. Mews* ————— **6865–6868**



Semiconductor Nanocrystals with
Adjustable Hole Acceptors: Tuning the
Fluorescence Intensity by Metal–Ion
Binding

Functional ligands: The fluorescence intensity of semiconductor nanocrystals (NCs) strongly depends on the energy level arrangement of the nanocrystals (the valence band (VB) and conducting band (CB)) and their molecular ligands. Using a functional ligand such as **1**, where the oxidation potential can be adjusted by metal–ion complexation, the fluorescence of the nanocrystals can be used for metal ion recognition.



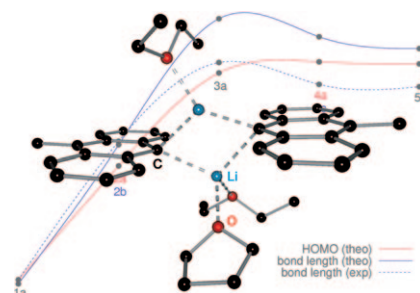
Organolithium Compounds

D. Stern, N. Finkelmeier, K. Meindl,
J. Henn, D. Stalke* ————— **6869–6872**



Consecutive Donor–Base Exchange in
Anthracenyllithium Compounds

Selective and consecutive donor–base addition and exchange in the same organolithium complex was monitored by structural determination, although it is feasible to fine-tune the composition of a mixed–base complex by stoichiometric addition of a second donor base. Remarkably, the length of the Li–C $_{\alpha}$ bonds is proportional to the reactivity as measured by frontier orbital energies with increasing amounts of the better donor base.



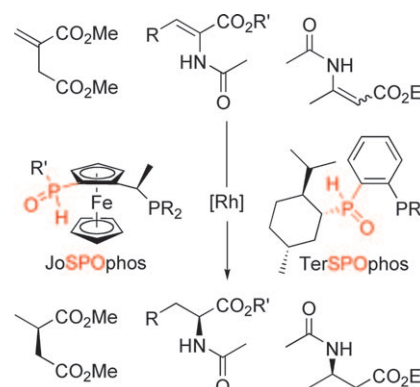
Ligand Design

H. Landert, F. Spindler, A. Wyss,
H.-U. Blaser, B. Pugin,* Y. Ribourduille,
B. Gschwend, B. Ramalingam,
A. Pfaltz* ————— **6873–6876**



Chiral Mixed Secondary Phosphine–
Oxide–Phosphines: High-Performing and
Easily Accessible Ligands for Asymmetric
Hydrogenation

P&O: Combining secondary phosphine oxides (SPOs) with phosphines leads to highly effective chiral bidentate ligands for transition-metal-based catalysts. JoSPOphos and TerSPOphos are readily accessible from inexpensive starting materials. The steric and electronic properties of these modular ligands can be easily tuned. In the asymmetric hydrogenation of functionalized alkenes, their rhodium complexes reacted to give enantioselectivities of up to 99% ee and turnover frequencies of up to 20000 h $^{-1}$.

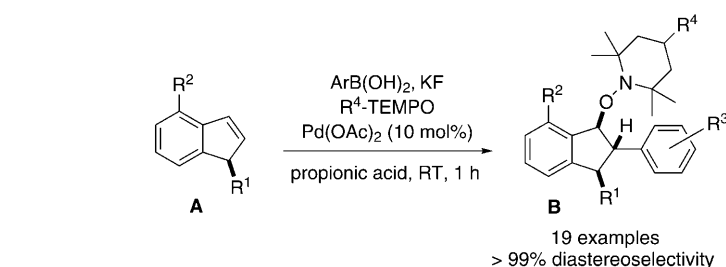


Oxyarylation

S. Kirchberg, R. Fröhlich,
A. Studer* ————— **6877–6880**

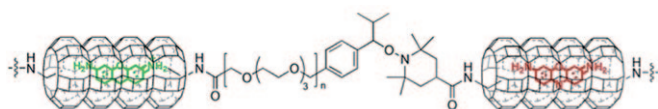


1,2,3-Trisubstituted Indanes by Highly
Diastereoselective Palladium-Catalyzed
Oxyarylation of Indenes with Arylboronic
Acids and Nitroxides



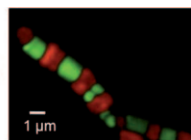
Excellent stereoselectivity is obtained in the synthesis of biologically interesting 1,2,3-trisubstituted indanes **B** by the reaction of readily prepared 3-substituted indenes **A** with commercially available

arylboronic acids by using various TEMPO derivatives as external oxidants and Pd-(OAc) $_2$ as a catalyst. The *anti,anti* isomers are formed and reactions occur stereospecifically under mild conditions.



Sticking together: The pore entrances of dye-loaded green or red zeolite L crystals can be site-specifically modified with either alkoxyamines or nitroxide radicals. Mild radical nitroxide exchange reactions of alkoxyamine-terminated “green” zeolite

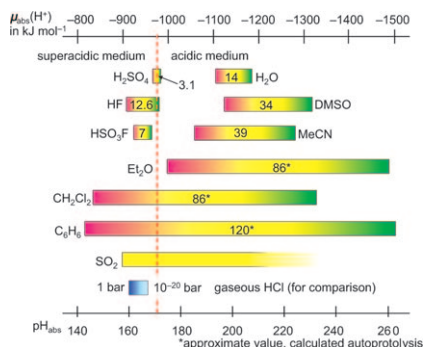
crystals with nitroxide-terminated “red” crystals leads to highly regular crystal chains that contain up to 15 covalently connected crystals with strictly alternating colors.



Surface Chemistry

B. Schulte, M. Tsotsalas, M. Becker, A. Studer,* L. De Cola* — 6881 – 6884

Dynamic Microcrystal Assembly by Nitroxide Exchange Reactions



One for all! On the basis of the absolute chemical potential of the proton, a unified absolute pH scale is introduced that is universally applicable in the gas phase, in solution, and in the solid state. With this scale, it is possible to directly compare acidities in different media, and to give a thermodynamically meaningful definition of superacidity. This scale can be used in all areas with variable proton activity.

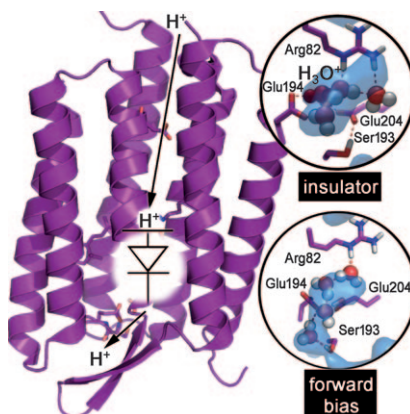
Acidity

D. Himmel, S. K. Goll, I. Leito, I. Krossing* — 6885 – 6888

A Unified pH Scale for All Phases



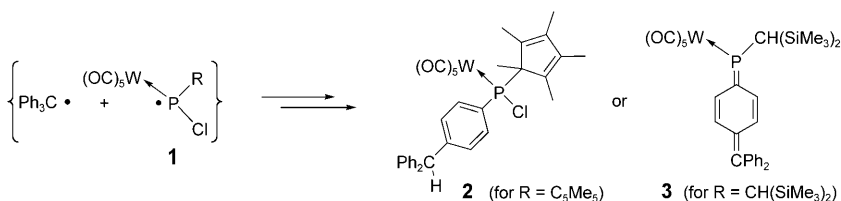
While proton transfer in liquid water is random, membrane proteins creating the proton gradient for ATP synthesis perform a directional proton transfer via protein-bound protonated water molecules. This was shown in bacteriorhodopsin by a combination of time-resolved FTIR spectroscopy, X-ray crystallography, and molecular dynamics simulations.



Structural Biology

S. Wolf, E. Freier, M. Potschies, E. Hofmann, K. Gerwert* — 6889 – 6893

Directional Proton Transfer in Membrane Proteins Achieved through Protonated Protein-Bound Water Molecules: A Proton Diode



C–P or C=P? One-electron oxidation of Li/Cl phosphinidenoid complexes led to the discovery of transient *P*-chlorophosphanyl complexes **1**. Subsequent cross-coupling and rearrangement or elimination reac-

tions yielded **2** and **3**; the latter is the first structurally characterized phosphaphino-methane complex. ESR spectroscopy and DFT calculations support the existence of short-lived P-centered radicals.

Functionalized Phosphanyl Complexes

A. Özbolat-Schön, M. Bode, G. Schnakenburg, A. Anoop, M. van Gastel,* F. Neese,* R. Streubel* — 6894 – 6898

Insights into the Chemistry of Transient *P*-Chlorophosphanyl Complexes



Cluster Compounds

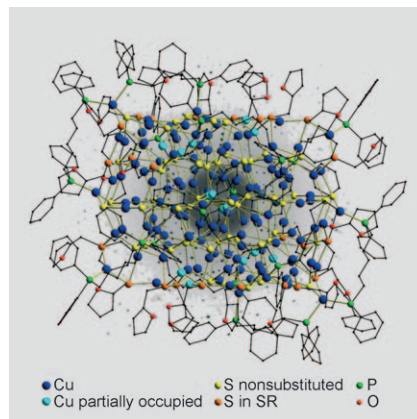
M.-L. Fu, I. Issac, D. Fenske,*
O. Fuhr* _____ **6899–6903**



Metal-Rich Copper Chalcogenide Clusters at the Border Between Molecule and Bulk Phase: The Structures of

$[\text{Cu}_{93}\text{Se}_{42}(\text{SeC}_6\text{H}_4\text{SMe})_9(\text{PPh}_3)_{18}]$,
 $[\text{Cu}_{96}\text{Se}_{45}(\text{SeC}_6\text{H}_4\text{SMe})_6(\text{PPh}_3)_{18}]$, and
 $[\text{Cu}_{136}\text{S}_{56}(\text{SCH}_2\text{C}_4\text{H}_3\text{O})_{24}(\text{dpppt})_{10}]$

Between molecule and bulk phase: The three title compounds are examples of ligand-stabilized clusters having significant structural features of the corresponding binary copper(I) chalcogenides. The cluster shown, $[\text{Cu}_{136}\text{S}_{56}(\text{SR})_{24}(\text{dpppt})_{10}]$, can be seen as an approximate $1.2 \times 1.4 \times 1.9 \text{ nm}^3$ section of a cubic phase of Cu_2S . The background shows a typical X-ray diffraction image of a single crystal of the cluster.



Supporting information is available on www.angewandte.org (see article for access details).



A video clip is available as Supporting Information on www.angewandte.org (see article for access details).

Sources

Product and Company Directory

You can start the entry for your company in “Sources” in any issue of *Angewandte Chemie*.

If you would like more information, please do not hesitate to contact us.

Wiley-VCH Verlag – Advertising Department

Tel.: 0 62 01 - 60 65 65

Fax: 0 62 01 - 60 65 50

E-Mail: MSchulz@wiley-vch.de

Service

Spotlight on Angewandte's

Sister Journals _____ **6704–6706**

Keywords _____ **6904**

Authors _____ **6905**

Vacancies _____ **6703**

Preview _____ **6907**

Corrigendum

Metal–Silicon Triple Bonds: The Molybdenum Silylidyne Complex $[\text{Cp}(\text{CO})_2\text{Mo}\equiv\text{Si-R}]$

A. C. Filippou,* O. Chernov,
K. W. Stumpf,
G. Schnakenburg _____ **3296–3300**

Angew. Chem. **2010**, 49

DOI 10.1002/anie.201000837

In the table of contents entry for this Communication the formula of the title compound was printed with a double bond instead of a triple bond. The correct formula is $[\text{Cp}(\text{CO})_2\text{Mo}\equiv\text{Si-R}]$.